Praise Worthy Prize

International Review on Computers and Software (I.RE.CO.S.), Vol. 5, N. 6
November 2010

Medical Image Compression Using Quincunx Wavelets and VQ Coding

M. Beladgham[1,2], A. Bessaid[1], A. Moulay-Lakhdar[2], A. Taleb-Ahmed[3]

Abstract –*In the field of medical diagnostics, interested parties have resorted increasingly to medical imaging. It is well established that the accuracy and completeness of diagnosis are initially connected with the image quality, but the quality of the image is itself dependent on a number of factors including primarily the processing that an image must undergo to enhance its quality. This paper introduces an algorithm for medical image compression based on the quincunx wavelets coupled with VQ coding algorithm, of which we applied the lattice structure to improve the wavelet transform shortcomings. In order to enhance the compression by our algorithm, we have compared the results obtained with those of other methods containing wavelet transforms. For this reason, we evaluated two parameters known for their calculation speed. The first parameter is the PSNR; the second is MSSIM (structural similarity) to measure the quality of compressed image. The results are very satisfactory regarding compression ratio, and the computation time and quality of the compressed image compared to those of traditional methods.*

Keywords: *Medical image, Compression, Quincunx wavelets, Lattice, VQ.*

Nomenclature

MRI	Magnetic Resonance Imaging
DCT	Discrete Cosine Transform
DWT	Discrete Wavelet Transform
VQ	Vector Quantization;
PSNR	Peak Signal to Noise Ratio
MSE	Mean Square Error
SSIM	The Structural Similarity Index
EZW	Embedded zerotree wavelet
SPIHT	Set Partitioning In Hierarchical Trees
CDF9/7	Cohen Daubechies-Feauveau wavelet

I. Introduction

The massive use of numerical methods in medical imaging (MRI, X scanner, nuclear medicine, etc…) today generates increasingly important volumes of data. The problem becomes even more critical with the generalisation of 3D sequence. So it is necessary to use compressed images in order to limit the amount of data to be stored and transmitted.

Among many compression schemes by transformation have been proposed, we can cite the standards JPEG images, MPEG 1 and 2 for compressing video. All of these standards are based on the discrete cosine transform (DCT) [1]. Over the past ten years, the wavelets (DWT), have had a huge success in the field of image processing, and have been used to solve many problems such as image compression and restoration [2].

However, despite the success of wavelets in various fields of image processing such as encoding, weaknesses have been noted in its use in the detection and representation of the objects' contours. The wavelets transform and other classical multi resolutions decompositions seem to form a restricted and limited class of opportunities for multi-scale representations of multidimensional signals.

To overcome this problem, we propose a new multi resolution decompositions by quincunx wavelets which are better adapted to the image representation. This structure of decomposition allows the construction of a no separable transform. No separable wavelets, by contrast, offer more freedom and can be better tuned to the characteristics of images. Their less attractive side is that they require more computations. The quincunx wavelets are especially interesting because they are nearly isotropic [3]. In contrast with the separable case, there is a single wavelet and the scale reduction is more progressive: one factor instead of 2.

In 1980, Gersho and Gray developed the vector quantization and many other researchers have been working on the research topic of VQ [4]-[5]-[6]. VQ is still one of the most successful signal processing techniques because it is quick and simple in decoding so that many applications that require fast decoding select this technique to compress data before transmission. Although this technique reduces image fidelity, it is still acceptable in many applications. Meanwhile having a high compression rate, the VQ method does not suffer from error propagation since

Manuscript received and revised October 2010, accepted November 2010

it is a fixed-length source coding technique. The image VQ coding steps are shown in part 5.

II. QUINCUNX WAVELETS

The separable dyadic analysis require three families of wavelets, which is sometimes regarded as a disadvantage, in addition the factor of addition between two successive scales is 4 which may seem high. It is possible to solve these two problems, but at the cost of the loss of filter separability and therefore a slightly higher computational complexity. An analysis has been particularly well studied to find a practical application, known as "quincunx" [1]. Quincunx decomposition results in fewer subbands than most other wavelet decompositions, a feature that may lead to reconstructed images with slightly lower visual quality. The method is not used much in practice, but [7] presents results that suggest that quincunx decomposition performs extremely well and may be the best performer in many practical situations. Figure (1) illustrates this type of decomposition [3].

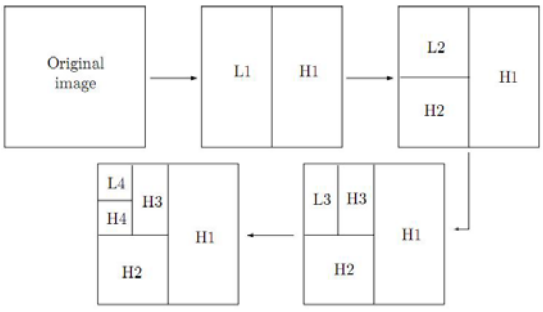

Fig. 1. Quincunx wavelet decomposition

We notice that the dilation factor is not more than 2 between two successive resolutions, and that only one wavelet family is necessary [8]-[9]. In this case the dilatation matrix will be: $M = \begin{bmatrix} 1 & 1 \\ 1 & -1 \end{bmatrix}$

The Grid transformation (lattice) is done according to the following diagram:

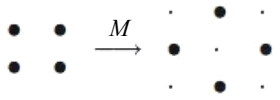

This matrix generates a quincunx lattice in 2D. The column vectors of this matrix form a basis to this lattice. The volume of the unit cell associated equals 2. The same lattice (Fig. 2) is also emanating from the matrix below [1]:

$$M' = \begin{bmatrix} 1 & -1 \\ 1 & 1 \end{bmatrix}$$

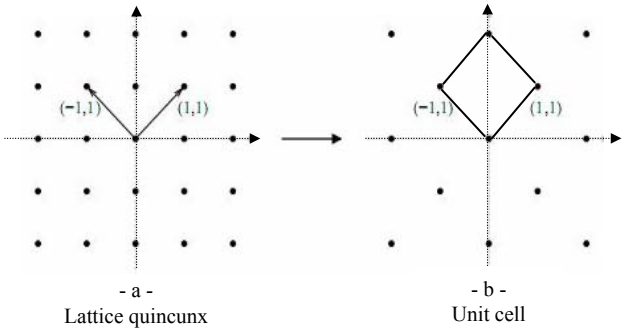

Fig. 2. Examples of a lattice quincunx and unit cell

It is noticed that the dilatation step is $\sqrt{2}$ on each direction and the geometry of the grid obtained justifies the name given to this multiresolution analysis.

III. Quincunx Sampling and Filter Banks

First, we recall some basic results on quincunx sampling and perfect reconstruction filter banks [10]-[11]. The quincunx sampling lattice is shown in figure 3. Let $x[\vec{n}]$ with $\vec{n} = (n_1, n_2) \in Z^2$ denote the discrete signal on the initial grid. The two-dimensional (2D) z-transform of $x[\vec{n}]$ is denoted by:

$$X(\vec{z}) = \sum_{\vec{n} \in Z^2} x[\vec{n}]\, \vec{z}^{-\vec{n}} \qquad (1)$$

Where:

$$\vec{z}^{\vec{n}} = \vec{z}^{n_1}\, \vec{z}^{n_2}$$

The continuous 2D Fourier transform is then given by $X(e^{j\vec{\omega}}) = \sum_{\vec{n} \in Z^2} x[\vec{n}] e^{-j(\vec{\omega},\vec{n})}$ with $\vec{\omega} = (\omega_1, \omega_2)$ and, finally, the discrete 2-D Fourier transform for $x[\vec{n}]$ given on an N x N grid $(n_1, n_2 = 0, 1, ..., N-1)$ by:

$$X[\vec{k}] = \sum_{\vec{n} \in Z^2} x[\vec{n}] e^{-j2\pi(\vec{k},\vec{n})/N},$$

With $(k_1, k_2 = 0, 1, ..., N-1)$

Now, we write the quincunx sampled version of $x[\vec{n}]$ as:

$$[x]_{\downarrow M}[\vec{n}] = x[M\,\vec{n}] \quad where \quad M = \begin{pmatrix} 1 & 1 \\ 1 & -1 \end{pmatrix} \qquad (2)$$

Our down-sampling matrix M is such that $M^2 = 2\,I$. where I is identity matrix.
The Fourier domain version of (1) is :

$$[x]_{\downarrow M}[\vec{n}] \leftrightarrow \frac{1}{2}\left[X(e^{jM^{-T}\vec{\omega}}) + X(e^{j(M^{-T}\vec{\omega}+\vec{\pi})})\right] \qquad (3)$$

Where:

$$\vec{\pi} = (\pi, \pi).$$

The up-sampling is defined by:

$$[x]_{\uparrow_M}[\vec{n}] = \begin{cases} x[M^{-1}\vec{n}], & when\ n_1 + n_2\ is\ even \\ 0 & elsewhere \end{cases} \quad (4)$$

and its effect in the Fourier domain is as follows:

$$[x]_{\uparrow_M}[\vec{n}] \longleftrightarrow X(e^{jM^T\vec{\omega}}) \quad (5)$$

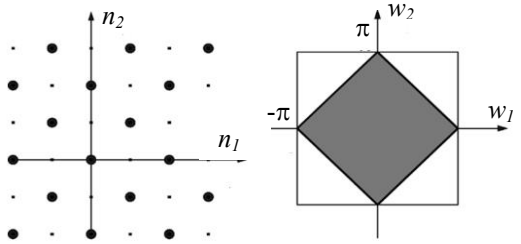

- a - - b -

Fig. 3. (a) Quincunx lattice, (b) the corresponding Nyquist area in the frequency domain

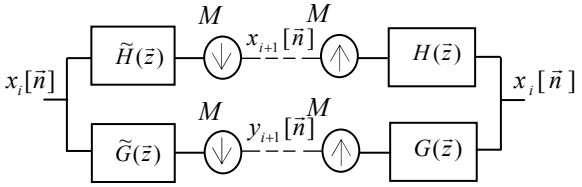

Fig.4. Perfect reconstruction filter bank on a quincunx lattice

If we now chain the down-sampling and up-sampling operators, we get

$$[x]_{\downarrow_M\uparrow_M}[\vec{n}] = \begin{cases} x[\vec{n}], & when\ n_1 + n_2\ is\ even \\ 0 & elsewhere \end{cases} \quad (6)$$

$$[x]_{\downarrow_M\uparrow_M}[\vec{n}] = \frac{1}{2}\left[X(e^{j\vec{\omega}}) + X(e^{j(\vec{\omega}+\vec{\pi})})\right] \quad (7)$$

Since quincunx sampling reduces the number of image samples by a factor of two, the corresponding reconstruction filterbank has two channels (Fig.4). The low-pass filter $\tilde{H}$ reduces the resolution by a factor of $\sqrt{2}$; the wavelet coefficients correspond to the output of the high-pass filter $\tilde{G}$.[8],[9], [10].

Applying the relation (7) to the block diagram in figure(4), it is easy to derive the conditions for a perfect reconstruction:

$$\begin{cases} \tilde{H}(\vec{z})H(\vec{z}) + \tilde{G}(\vec{z})G(\vec{z}) = 2 \\ \tilde{H}(-\vec{z})H(\vec{z}) + \tilde{G}(-\vec{z})G(\vec{z}) = 0 \end{cases} \quad (8)$$

Where H and G (respectively $\tilde{H}$ and $\tilde{G}$) are the transfer functions of the synthesis (respectively analysis) filters. In the orthogonal case, the analysis and synthesis filters are identical up to a central symmetry; the wavelet filter G is simply a modulated version of the low-pass filter H .

IV. Fractional Quincunx Filters

To generate quincunx filters, we will use the standard approach which is to apply the diamond McClellan transform to map a 1D design onto the quincunx structure [14].

IV.1. New 1D Wavelet Family

As starting point for our construction, we introduce a new 1-D family of orthogonal filters:

$$H_\alpha(z) = \frac{\sqrt{2}\,(z+2+z^{-1})^{\frac{\alpha}{2}}}{\sqrt{(z+2+z^{-1})^{\alpha} + (-z+2-z^{-1})^{\alpha}}} \quad (9)$$

$$H_\alpha(\omega) = \frac{\sqrt{2}\,(2+2\cos\omega)^{\frac{\alpha}{2}}}{\sqrt{(2+2\cos\omega)^{\alpha} + (2-2\cos\omega)^{\alpha}}} \quad (10)$$

which is indexed by the continuously-varying order parameter α.

These filters are symmetric and are designed to have zeros of order α at $z=-1$; the numerator is a fractional power of $(z+2+z^{-1})$ (the simplest symmetric refinement filter of order 2) and the denominator is the appropriate L2-orthonormalization factor. Also note that these filters are maximally flat at the origin; they essentially behave $H_\alpha(z)/\sqrt{2} = 1 + O(\omega^\alpha)$ as $\omega \to 0$. Their frequency response is similar to the Daubechies' filters with two important differences: 1) the filters are symmetric and 2) the order is not restricted to integer values.[8],[9]

IV.2. Corresponding 2D Wavelet Family

Applying the diamond McClellan transform to the filter above is straightforward; it amounts to replacing $\cos\omega$ by $(1/2)(\cos\omega_1 + \cos\omega_2)$ in (10). Thus, our quincunx refinement filter is given by:

$$H_\alpha(e^{j\vec{\omega}})=\frac{\sqrt{2}\,(2+\cos\omega_1+\cos\omega_2)^{\frac{\alpha}{2}}}{\sqrt{\left[\begin{matrix}(2+\cos\omega_1+\cos\omega_2)^{\alpha}+\\(2-\cos\omega_1-\cos\omega_2)^{\alpha}\end{matrix}\right]}} \quad (11)$$

This filter is guaranteed to be orthogonal because the McClellan transform has the property of preserving biorthogonality. Also, by construction, the α th order zero at $\omega=\pi$ gets mapped into a corresponding zero at $(\omega_1,\omega_2)=(\pi,\pi)$; this is precisely the condition that is required to get a 2-D wavelet transform of order α. Also, note the isotropic behavior and the flatness of $H_\alpha(e^{j\vec{\omega}})$ around the origin; i.e, $H_\alpha(e^{j\vec{\omega}})/\sqrt{2}=1+O(\|\vec{\omega}\|^\alpha)$ for $\vec{\omega}\to 0$. The orthogonal wavelet filter is obtained by modulation :

$$G_\alpha(\vec{z})=z_1 H_\alpha(-\vec{z}^{-1}) \quad (12)$$

The corresponding orthogonal scaling function is defined implicitly as the solution of the quincunx two-scale relation:

$$\varphi_\alpha(\vec{x})=\sqrt{2}\sum_{\vec{n}\in Z^2} h_\alpha[\vec{n}]\,\varphi_\alpha(M\vec{x}-\vec{n}) \quad (13)$$

Since the refinement filter is orthogonal with respect to the quincunx lattice, it follows that $\varphi_\alpha(\vec{x})\in L_2(R^2)$ and that it is orthogonal to its integer translates. Moreover, for $\alpha>0$, it will satisfy the partition of unity condition, which comes as a direct consequence of the vanishing of the filter at $(\omega_1,\omega_2)=(\pi,\pi)$ Thus, we have the guarantee that our scheme will yield orthogonal wavelet bases of $L_2(R^2)$. The underlying orthogonal quincunx wavelet is simply:

$$\psi_\alpha(\vec{x})=\sqrt{2}\sum_{\vec{n}\in Z^2} g_\alpha[\vec{n}]\,\varphi_\alpha(M\vec{x}-\vec{n}) \quad (14)$$

V. Vector Quantization

In VQ, the image is divided into small non-overlapping blocks. E.g. 4x4 pixel blocks are considered as vectors of dimension 16. At the encoder, each vector $\mathbf{x_i}$ of the image is compared to the elements of a codebook $W=\{\mathbf{w_0},\mathbf{w_1},...,\mathbf{w_{N-1}}\}$, called the codevectors or codewords, and only the index of the nearest codevector is transmitted. The best matching codevector is selected according to some distortion measure, which is in general the mean square error. The decoder reconstructs the signal by simply performing table-lookup operation to fetch codevectors from a codebook which is identical to that of the encoder. The encoding and decoding scheme is shown in Fig.5.

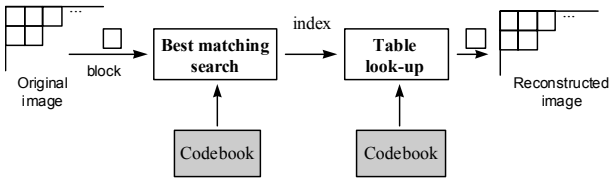

Fig. 5. VQ encoder and decoder

The codebook must contain vectors that represent well the images to be compressed. Several methods are used in constructing codebooks. They apply, in general, a learning method on the training set issued from available images which are supposed to be representative of the images to be compressed.

VI. Image Coding Application

VI.1. Compression Quality Evaluation

The Peak Signal to Noise Ratio (PSNR) is the most commonly used as a measure of quality of reconstruction in image compression. The PSNR were identified using the following formulae:

$$MSE=\frac{1}{MxN}\sum_{1=1}^{i=N}\sum_{j=1}^{j=M}\left(I(i,j)-\hat{I}(i,j)\right)^2 \quad (15)$$

Mean Square Error (MSE) which requires two *M*x*N* grayscale images I and $\hat{I}$ where one of the images is considered as a compression of the other is defined as:

- The PSNR is defined as:

$$PSNR=10\log_0\left(\frac{(Dynamics\ \ of\ \ image)^2}{MSE}\right) \quad (16)$$

Usually an image is encoded on 8 bits. It is represented by 256 gray levels, which vary between 0 and 255, the extent or dynamics of the image is 255.

- The structural similarity index (SSIM):

The PSNR measurement gives a numerical value on the damage, but it does not describe its type. Moreover, as is often noted in [16],[17], it does not quite represent the quality perceived by human observers. For medical imaging applications where images are degraded must eventually be examined by experts, traditional evaluation remains insufficient. For this reason, objective approaches are needed to assess the medical imaging quality. We then evaluate a new paradigm to estimate the quality of medical images, specifically the ones compressed by wavelet transform, based on the assumption that the human visual system (HVS) is highly adapted to extract structural information. The similarity compares the brightness, contrast and structure between each pair of vectors, where the structural similarity

index (SSIM) between two signals x and y is given by the following expression [18],[19]:

$$SSIM(x,y)=l(x,y).c(x,y).s(x,y) \quad (17)$$

Finally the quality measurement can provide a spatial map of the local image quality, which provides more information on the image quality degradation, which is useful in medical imaging applications. For application, we require a single overall measurement of the whole image quality that is given by the following formula:

$$MSSIM(I,\hat{I})=\frac{1}{M}\sum_{i=1}^{M}SSIM(I_i,\hat{I}_i) \quad (18)$$

Where I and $\hat{I}$ are respectively the reference and degraded images, I_i and $\hat{I}_i$ are the contents of images at the i-th local window.

M: the total number of local windows in image. The MSSIM values exhibit greater consistency with the visual quality.

VI.2. Algorithm

In this paper, the given image, the original image is transformed based on the quincunx wavelets, up to three levels of decomposition. The resulting transform coefficients are encoded using unstructured, full-search VQ. The codebook has been designed using the iterative LBG algorithm and it has been initialized using the splitting technique. The medical images have been used for testing. Quincunx wavelets coefficients at each resolution for every level of decomposition are encoded with a separate codebook. At each resolution, tow subcodebooks have been designed for encoding each detail separately. The codebooks have been designed with a sample training set of four images. The minimum size of the subcodebook designed is 4 and the maximum size is 2048. The size of the codebook becomes optimal, when there is not much increase in PSNR with increase in codebook size. The number of bits required for each code vector is $\lceil \log 2M \rceil$ bits where M is the size of the respective subcodebook. The decoder uses the same set of codebooks as at the encoder. The encoder-decoder will work for any image within the training set used to design the codebook. If the training set is extended, it can be used for other images outside the set also. Designing the same codebook at the receiver makes it unnecessary to transmit the codebook along with the image. The reproduction code vectors for each of the indices transmitted are concatenated to form the reproduction matrix of the quincunx wavelets coefficients of the image. The inverse quincunx wavelets transform is then applied to reconstruct the image. The most important low frequency information present in the approximation subband is coded first.

Then the details are coded, in that order. This process is repeated for every resolution in the case of level 3 decompositions. The encoding / decoding can be terminated at any time, with the best reproduction obtained up to that point. This is made possible because of the progressive nature of the coding algorithm.

VII. Results and Discussion

We are interested in lossy compression methods based on 2D wavelet transforms because of their interesting properties. Indeed, the 2D wavelet transforms combines good spatial and frequency locations. As we work on medical image, the spatial location and frequency are important [19],[20].

In this article we have applied our algorithm to compress medical images. For this reason we have chosen an axial slice of human brain size 512x512 (grayscale), encoded on 8 bits per pixel, and recorded by means of an MRI scanner. This image is taken from the GE Medical System database [21]. The codebook we used to encode this images was yielded LBG with the size of 256 code-vector. The bits to represent each index are eight. Each indice is the index for a 4 by 4 code-vector in the codebook.

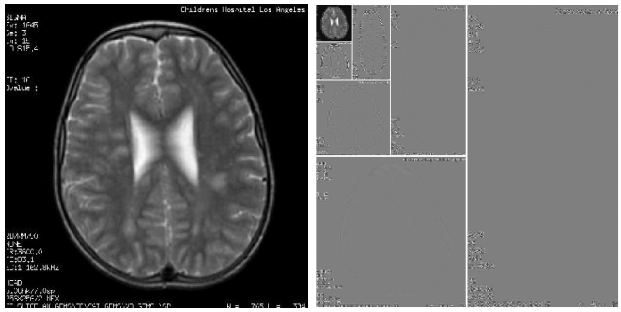

- a - Axial slice

- b - Quincunx wavelet decomposition

Fig. 6. Original image

The importance of our work lies in the possibility of reducing the rates for which the image quality remains acceptable. Estimates and judgments of the compressed image quality is given by the PSNR evaluation parameters and the MSSIM similarity Index.

Figure (7) shown below illustrates the compressed image quality for different bit-rate values (number of bits per pixel). According to the PSNR and MSSIM values, we note that from 0.5bpp, image reconstruction becomes almost perfect.

To show the performance of the proposed method, we make a comparison between these different types of transform: Quincunx wavelet and QV coding, (CDF 9/7 (Filter Bank) and CDF9/7 (Lifting scheme)) coupled with the SPIHT coding and CDF9/7 (Lifting scheme) combined with the EZW coding.

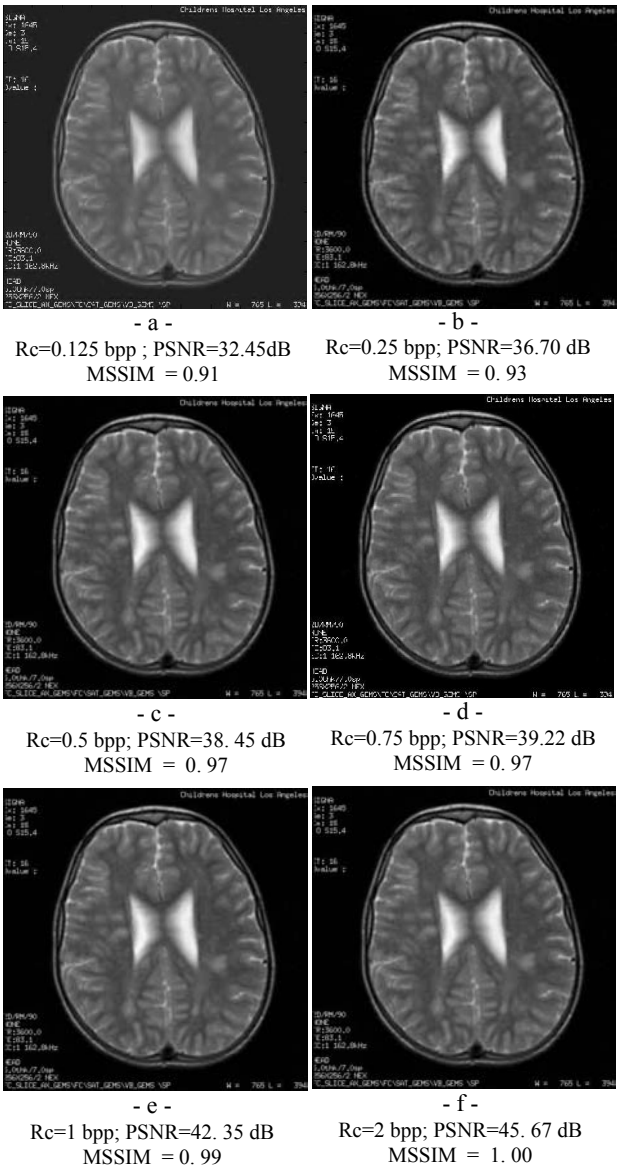

- a -
Rc=0.125 bpp ; PSNR=32.45dB
MSSIM = 0.91

- b -
Rc=0.25 bpp; PSNR=36.70 dB
MSSIM = 0. 93

- c -
Rc=0.5 bpp; PSNR=38. 45 dB
MSSIM = 0. 97

- d -
Rc=0.75 bpp; PSNR=39.22 dB
MSSIM = 0. 97

- e -
Rc=1 bpp; PSNR=42. 35 dB
MSSIM = 0. 99

- f -
Rc=2 bpp; PSNR=45. 67 dB
MSSIM = 1. 00

Fig. 7. Compressing of an axial slice with Quincunx wavelet and QV coding

For each application we vary the bit-rate 0.125 to 2 and calculate the PSNR and MSSIM. The results obtained are given in TableI and TableII.

The comparison in terms of image quality for the four algorithms is given by the PSNR and MSSIM curves represented in figures 8 and 9.

TABLE I
RESULTS

R_c (bpp)	Quincunx wavelet + QV		CDF9/7 (Lifting) + SPIHT	
	PSNR	MSSIM	PSNR	MSSIM
0.125	32.45	0.91	19.79	0.59
0.25	36.70	0.93	25.74	0.76
0.5	38.45	0.97	34.95	0.91
0.75	39.22	0.97	40.74	0.97
1	42.35	0.99	45.03	0.99
1.5	43.87	0.99	50.76	1.00
2	45.67	1.00	55.17	1.00

TABLE II
RESULTS

R_c (bpp)	CDF9/7(Filter bank) + SPIHT		CDF9/7 (Lifting) + EZW	
	PSNR	MSSIM	PSNR	MSSIM
0.125	18.38	0.59	19.44	0.58
0.25	23.62	0.63	22.65	0.70
0.5	32.22	0.80	29.85	0.82
0.75	37.88	0.89	34.61	0.90
1	42.32	0.95	37.93	0.94
1.5	48.07	0.98	43.27	0.98
2	52.19	0.99	46.77	0.99

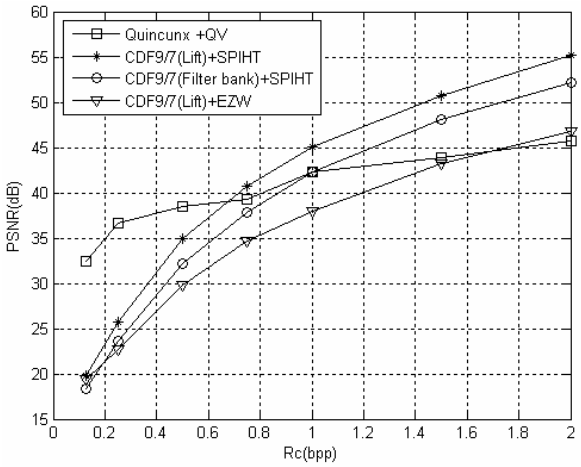

Fig. 8. PSNR variation using different methods

Comparing the different values of PSNR and MSSIM, we show clearly the efficiency of our algorithm in terms of compressed image quality for the low bit-rate.

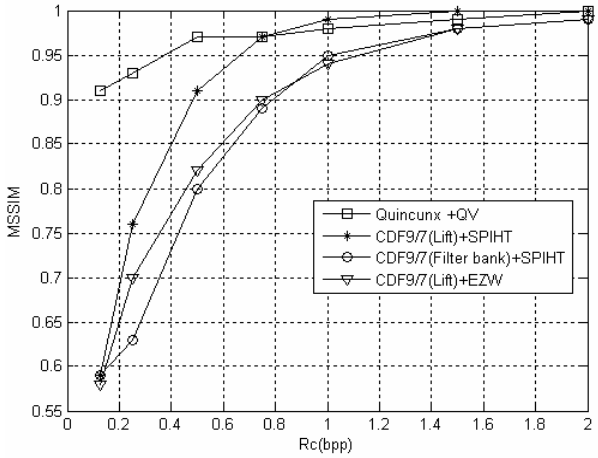

Fig. 9. MSSIM variation using different methods

This study was subsequently generalized to a set of medical images of the GE Medical Systems database. The following figure presents the results obtained after application of different algorithms on an axial slice of body imaging. These results are obtained with a 0.5-bpp bit-rate.

Original Image

Quincunx wavelet +QV
PSNR=35.75 dB ; MSSIM=0.92

CDF9/7 (Lifting)+SPIHT
PSNR=35.43 dB; MSSIM=0.92

CDF9/7 (Filter Bank)+SPIHT
PSNR=32. 81 dB; MSSIM=0.85

CDF9/7 (Lifting)+EZW
PSNR=30.93 dB; MSSIM=0.85

Fig. 10. Axial slice of Body imaging (CT)

The following figures present a set of medical images (MRI) from GE Healthcare database[22] (GE Healthcare), compressed by the quincunx wavelets algorithm for a 0.5-bpp bit-rate.

Patient - Male
Age - 52 years
Exam performed with CTL coil
Sag FRFSE-XL T2 4mm
Patient in serious aggravation
Plaque of demyelinization, multiple sclerosis

Original Image (512x512)

Quincunx wavelet +QV
PSNR=34.43 dB; MSSIM= 0.95

Fig. 11. Neuro imaging

Patient - Female
Age - 45 years
Intra-articular effusion
Exam acquired with the Head coil.
Sag T2 GRE 3mm

Original Image (512x512)

Quincunx wavelet +QV
PSNR=37.23 dB; MSSIM= 0.98

Fig. 12. Orthopedic imaging

We can say that our compression algorithm better preserves the different image structures for bit-rates higher or equal to 0.5 bpp.

VIII. Conclusion

The objective of this paper is undoubtedly the enhancement of medical images quality after the compression step. The latter is regarded as an essential tool to aid diagnosis (storage or transmission) in medical imaging. We used the quincunx wavelet compression coupled with the QV coding. After several applications, we found that this algorithm gives better results than the other compression techniques.

To develop our algorithm, we used various types of medical images. We have noticed that for 0.5 bpp bit-rate, the algorithm provides very important PSNR and MSSIM values for MRI images. Therefore, at high bit-rate our algorithm is less efficacy then other methods. Thus, we conclude that the results obtained are very satisfactory in terms of compression ratio and compressed image quality.

In perspective, we aspire to apply our algorithm to compress video sequences.

References

[1] V. Chappelier, Progressive coding of images by directed wavelet. *Phd Thesis*, Rennes1University, 2005.

[2] S. Mallat, Multifrequency channel decompositions of images and wavelet models. *Transaction in Acoustic Speech and Signal Processing (IEEE)*, vol. 37, 1989, pp. 2091-2110.

[3] D. Salomon, Data ompression. The Complete Reference, (Third Edition, Springer).

[4] Y.G. Wu, K.L. Fan, Fast vector quantization image coding by mean value predictive algorithm, *J.Electron.Imaging, vol. 2 n.*13, 2004, pp.324–333.

[5] Y.G. Wu, Design of a fast vector quantization image encoder, *Opt.En, vol. 8 n.46* , 2007, pp. 08700801–08700812.

[6] K. Sayood, Introduction to Data Compression, Morgan Kaufman, (San Francisco, CA,USA, 2000).

[7] Stromme, Oyvind. On The Applicability of Wavelet Transforms to Image and Video Compression. *Ph.D. thesis, University of Strathclyde*, 1999.
[8] F. Truchetet, Wavelts for digital signal. Hermes Edition. (*Paris*, 1998).
[9] Y. Tanaka, M. Ikehara and Q.N. Truong, A New Combination of 1D and 2D Filter Banks for Effective Multiresolution Image Representation. *IEEE*, 2008, pp.2820-2823.
[10] M. Vetterli, J. Kovacevé, Wavelets and Subband Coding. *Upper Saddle River*,(NJ: Prentice-Hall, 1995).
[11] F. Manuela, VD. Dimitri and U. Michael, An Orthogonal Family of Quincunx Wavelets With Continuously Adjustable Order. *IEEE Transactions On Image Processing,* vol. 14, n. 4, 2005.
[12] VD. Dimitri, B. Thierry and U. Michael, On the Multidimensional Extension of the Quincunx Subsampling Matrix. *IEEE Signal Processing Letters, vol. 12, n. 2*, 2005.
[13] Y. Chen, AD. Michael and L. Wu-Sheng, Design of Optimal Quincunx Filter Banks for Image Coding. *Journal on Advances in Signal Processing (EURASIP)*, 2007.
[14] L. Lee, V. A .Oppenheir, Proprerties of approximate parks-McClellan filters. *IEEE,* 1997, pp. 2165-2168.
[15] W. S. Geisler, M. S. Banks, Visual performance. *in Handbook of Optics (M. Bass, ed.),*(McGraw-Hill,1995).
[16] A. B. Watson, L. Kreslake, Measurement of visual impairment scales for digital video. *in Human Vision, Visual Processing, and Digital Display, Proc. (SPIE), vol. 4299*, 2001.
[17] Z. Wang, A. C. Bovik, H. R. Sheikh and E.P. Simoncelli, Image quality assessment:From error visibility to structural similarity. *IEEE Transactions on Image Processing, vol. 13, n. 4*.2004.
[18] Z.Wang, A. C. Bovik, A universal image quality index. *Signal Processing Letters(IEEE), vol. 9*, 2002, pp.81–84.
[19] R.W. Buccigrossi, E.P. Simoncelli, Image compression via joint statistical characterization in the wavelet domain. *IEEE Trans. Image Processing, vol. 8*, 1999,pp.1688–1701.
[20] D.M. Chandler, S.S. Hemami, Additivity models for suprathreshold distortion in quantized wavelet-coded images. *in Human Vision and Electronic Imaging VII, Proc. (SPIE)*, *vol. 4662*, 2002.
[21] www.GE Medical System.com (database).
[22] www. GE Healthcare.com (database).

Authors' information

[1,2] Genie-Biomedical Laboratory, Departement of Electronics Abou bekr Belkaid university,Tlemcen, 13000, Algeria
[2] Bechar University, 08000, Algeria.
[3] Biomecanic Laboratory, Valencienne University, France
E-mail*: beladgham@yahoo.fr*

BELADGHAM Mohammed obtained the Engineer degree in Electronics from university of Tlemcen, Algeria, and then a Magister in signals and systems from university of Tlemcen, Algeria. His research interests are Image processing, Medical image compression, wavelets transform and optimal encoder**.**